Coherent Synchrotron Radiation in Whispering Gallery Modes: Theory and Evidence

R. Warnock, SLAC National Accelerator Laboratory

Many thanks to Jack Bergstrom, Steve Kramer, and Larry Carr

October 14, 2010

HISTORY

Lord Rayleigh (John William Strutt, 3rd Baron Rayleigh [1842-1919]), "The Theory of Sound, Vol. 2" (1896):

"One of the most striking of the phenomena connected with the propagation of sound within closed buildings is that presented by "whispering galleries", of which a good and easily accessible example is to be found in the circular gallery at the base of the dome of St. Paul's cathedral"

Figure: St. Paul's Cathedral, London. Architect: Sir Christopher Wren

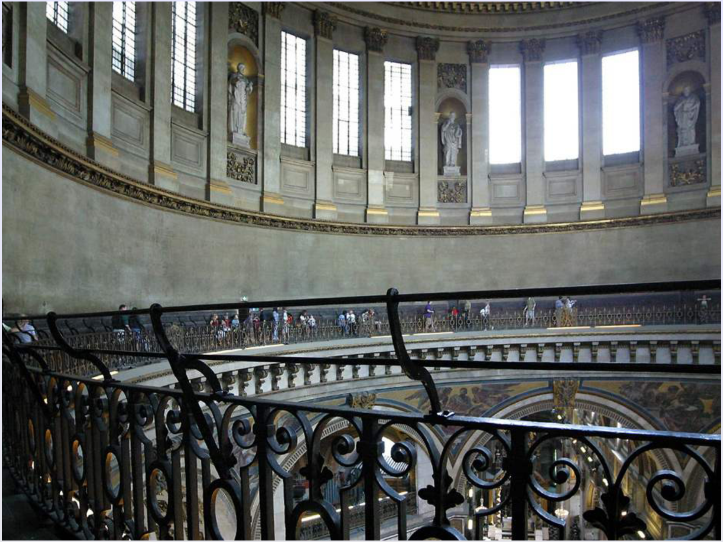

Figure: Whispering Gallery in St. Paul's Cathedral

Rayleigh's View

"In the opinion of the Astronomer Royal (Sir George Biddell Airy [1801-1892]) the effect is to be ascribed to reflection from the surface of the dome overhead, and is to be observed at the point of the gallery diametrically opposite to the source of sound"

"Judging from some observations that I have made in St. Paul's whispering gallery, I am disposed to think that the principal phenomenon is to be explained somewhat differently. The abnormal loudness with which a whisper is heard is not confined to the position diametrically opposite to that occupied by the whisperer ...."

Rayleigh's experiment - 1

"The whisper seems to creep around the gallery horizontally, not necessarily along the the shorter arc, but rather along that arc toward which the whisperer faces"

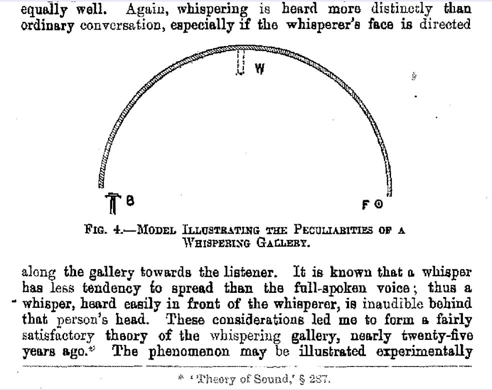

equally well. Again, whispering is heard more distinctly than ordinary conversation, especially if the whisperer's face is directed

FIG. 4.—MODEL ILLUSTRATING THE PECULIARITIES OF A WHISPERING GALLERY.

along the gallery towards the listener. It is known that a whisper has less tendency to spread than the full-spoken voice; thus a whisper, heard easily in front of the whisperer, is inaudible behind that person's head. These considerations led me to form a fairly satisfactory theory of the whispering gallery, nearly twenty-five years ago.* The phenomenon may be illustrated experimentally

* 'Theory of Sound,' § 287.

"Especially remarkable is the narrowness of the obstacle, held close to the concave surface, which is competent to intercept most of the effect."

Rayleigh's Experiment -2

434 *Lord Rayleigh on Shadows.* [Jan. 15,

by the small scale arrangement represented diagrammatically in Fig. 4. A strip of zinc, about 2 feet wide and 12 feet long, is bent into the form of a semicircle; this forms the model of the whispering gallery. The bird-call B is adjusted so that it throws the sound tangentially against the inner surface of the zinc: it thus takes the place of the whisperer. The sensitive flame F takes the place of the listener. A flame is always more sensitive to sound reaching it in one direction than in others; the flame F is therefore adjusted so that it is sensitive to sounds leaving the gallery tangentially. The flaring of the flame shows that sound is reaching it: if an obstacle is interposed in the straight line F B the flame flares as before; but if a lath of wood W, which need not be more than 2 inches wide, is placed against the inner surface of the zinc, the flame recovers, showing that the sound has been intercepted. Thus the sound creeps round the inside surface of the zinc, and there is no disturbance except at points within a limited distance from that surface.

[R.]

Figure: Proc. Royal Institution Great Britain, January, 1904

Rayleigh's Ray Picture

Suppose that a source near the wall emits sound with a maximum angular spread of θ. The higher the frequency the smaller the angle θ. Then in a ray picture, the minimum distance of a ray from the center is $b\cos\theta$

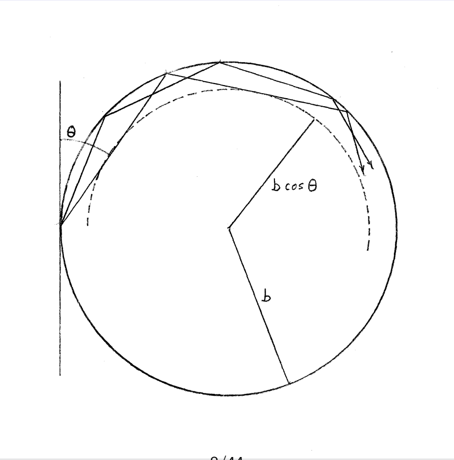

Rayleigh's Wave Theory

"The Problem of the Whispering Gallery", Phil. Mag. **20**, 1001, (1910)

"I have often wished to illustrate the matter further on distinctly wave principles, but only recently have recognized that most of what I sought lay as it were under my nose. The mathematical solution in question is very simple in form, although the reduction to numbers, in the special circumstances, presents certain difficulties."

Analysis of transmissive wall:

"Further Applications of Bessel's Functions of High Order to the Whispering Gallery and Allied Problems", Phil. Mag. **27**, 100 (1914).

Rayleigh's wave theory - 2

$\mathbf{v} = \nabla\psi =$ velocity field
$\psi =$ velocity potential

$$\triangle\psi - \frac{1}{v^2}\frac{\partial^2\psi}{\partial t^2} = 0 \tag{1}$$

Elementary solution:

$$\psi = J_n(kr)cos(kvt - n\theta) \tag{2}$$

Boundary condition: radial velocity $v_r = \partial\psi/\partial r$ must be zero on boundary $r = b$:

$$J'_n(kb) = 0 \quad \Rightarrow \quad kb = j'_{ns}, \quad s = 1, 2, \cdots \tag{3}$$

Rayleigh's wave theory - Eigensolution

$$\psi_{ns}(r,\theta,t) = J_n(\frac{j'_{ns} r}{b}) \cos(\frac{j'_{ns} v}{b} t - n\theta)$$
$$\text{frequency} = \omega = \frac{j'_{ns} v}{b} \quad \text{(dispersion relation)} \tag{4}$$

Basic property of Bessel functions $J_n(nz)$, $J'_n(nz)$- Transition:

- Cuts off exponentially as z decreases from 1.
- Oscillates as z increases from 1.

Compare to transition of harmonic oscillator:

$$J''_n(x) + \frac{1}{x} J'_n(x) + (1 - \frac{n^2}{x^2}) J_n(x) = 0, \quad y''(t) + \omega^2 y(t) = 0 \ . \tag{5}$$

Thus j'_{n1} is slightly larger than n, and for r slightly less than b, the eigensolution ψ_{n1} is negligible!

Quantitative treatment of concentration near boundary (large n):

Cut-off of $J_n(nz)$ for $z < 1$ and large n comes from factor $\exp(-n\xi)$, where $\xi \approx (1 - z^2)^{3/2}/3$. Thus down by factor $1/e$ at

$$z = 1 - \frac{1}{2}\left[\frac{3}{n}\right]^{2/3} . \tag{6}$$

Our wave function $J_n(j'_{ns} r/b)$ down by $1/e$ for

$$\frac{r}{b} = \frac{n}{j'_{ns}}\left[1 - \frac{1}{2}\left[\frac{3}{n}\right]^{2/3}\right] = 1 - 2^{-1/3}\left(|a'_s| + (3/2)^{2/3}\right) n^{-2/3}, \tag{7}$$

where a'_s is the s-th negative zero of $Ai'(x)$. (From Olver's asymptotic expansion of j'_{ns}, uniform in s.)

Concentration near boundary:

$$b - r = 2^{-1/3}\left(|a'_s| + (3/2)^{2/3}\right) n^{-2/3} b \tag{8}$$

$$\begin{aligned} a'_1 &= -1.0187\ ,\ a'_2 = -3.2481\ ,\cdots \\ a'_s &\sim -\Big[\frac{3\pi}{8}(4s-3)\Big]^{2/3}\ ,\ s \to \infty\ . \end{aligned} \tag{9}$$

The higher the frequency, the sharper the concentration near the boundary! This is in accord with the ray theory, since the higher the frequency the smaller the maximum angle θ of emitted rays:

$$b - r = b(1 - \cos\theta)\ . \tag{10}$$

CSR in Storage Rings - Toroidal Vacuum Chamber

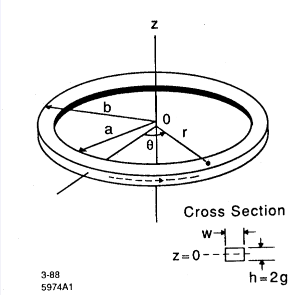

Solve for longitudinal electric field $E_\theta(r, \theta, z, t)$ produced by the beam at the position of beam ($r = R\ , z = 0$), the Wake Field, which determines the dynamics of the bunch. The work done by the wake field per unit time is the negative of the Radiated Power.

Since the field is concentrated near $r = b$, the result is nearly the same for a "pillbox" chamber with $a = 0$. Let's give equations for pillbox.

Solution in Terms of Bessel Functions - 1

R. W. and P. Morton, "Fields Excited by a Beam in a Toroidal Vacuum Chamber", SLAC-PUB-4562 (1988), Part. Accel. **25**, 113 (1990). Cited as W & M in following.

Write Maxwell's equations for Laplace-Fourier transforms of field components, e.g.,

$$\begin{aligned}\widehat{E}_z(r,n,p,\omega) &= \frac{1}{2\pi}\int_0^{2\pi} d\theta\ e^{-in\theta}\frac{1}{g}\int_{-g}^{g} dz\ \cos(\alpha_p(z+g)) \\ &\cdot\frac{1}{2\pi}\int_0^{\infty} dt\ e^{i\omega t}E_z(r,\theta,z,t)\ ,\end{aligned}\tag{11}$$

where $\alpha_p = \pi p/h$ and $\mathrm{Im}\ \omega > 0$. The usual Laplace variable is $s = -i\omega$. Fourier transform in time won't do, because fields do not decay at large t!

All fields can be expressed algebraically in terms of $\widehat{E}_z, \widehat{H}_z$ and their r-derivatives. Also, $\widehat{E}_z, \widehat{H}_z$ satisfy Bessel equations in r, with sources.

Solution in Terms of Bessel Functions - 2

Boundary conditions on the top and bottom walls met by right choice of Fourier series in z, and on the cylindrical wall by the right linear combination of Bessel solutions.

Assume charge density of the form

$$\rho(r,\theta,z,t) = q\lambda(\theta-\omega_0 t)H(z)\frac{\delta(r-R)}{R}\ . \tag{12}$$

(Rigid bunch, vertical ribbon, zero emittance).

Since the inhomogeneous Bessel equation can be solved for any source, this restriction can be lifted.

$$\hat{\rho}(n,p,\omega,r) = \frac{qH_p\lambda_n}{2\pi i(\omega-n\omega_0)}\frac{\delta(r-R)}{R}\ . \tag{13}$$

Solution for longitudinal field - 1

$$
\begin{aligned}
&\hat{E}_\theta(r,n,p,\omega) = -\frac{q\beta c Z_0 \lambda_n}{4(\omega - n\omega_0)} \\
&\cdot\left[\frac{\omega}{c}\left(\frac{J_n'(\gamma_p r)}{J_n'(\gamma_p b)} s_n(\gamma_p b, \gamma_p R) + \theta(r-R) s_n(\gamma_p r, \gamma_p R)\right)\right. \\
&\left. + \frac{n}{\beta R}\left(\frac{\alpha_p}{\gamma_p}\right)^2 \left(\frac{J_n(\gamma_p r)}{J_n(\gamma_p b)} p_n(\gamma_p b, \gamma_p R) + \theta(r-R) p_n(\gamma_p r, \gamma_p R)\right)\right] \\
&\gamma_p^2 = (\omega/c)^2 - \alpha_p^2 \ , \quad \alpha_p = \pi p/h \ , \\
&p_n(x,y) = J_n(x) Y_n(y) - Y_n(x) J_n(y) \ , \\
&s_n(x,y) = J_n'(x) Y_n'(y) - Y_n'(x) J_n'(y)
\end{aligned} \tag{14}
$$

Displays the same concentration near the outer wall as in Rayleigh's case and similar resonances!

Whispering Gallery Resonances

Resonances result from boundary conditions, as in Rayleigh theory, and give poles in the ω-plane:

$$J_n'(\gamma_p b) = 0 \quad (TE)\ , \quad J_n(\gamma_p b) = 0 \quad (TM)\ ,$$
$$\gamma_p^2 = (\omega/c)^2 - (\pi p/h)^2\ . \tag{15}$$

Unusual nomenclature: TE and TM fields transverse to z-axis (vertical)

Radial wave functions similar for torus and pillbox:

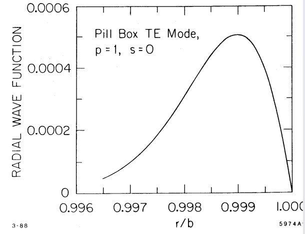

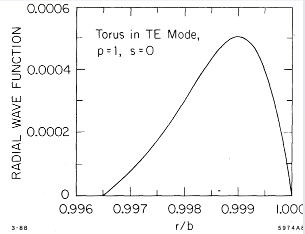

Here $s = 0$ is $s = 1$ in present notation.

Solution for longitudinal field - 2

The field (averaged over transverse distributions) can be expressed in terms of the impedance $Z(n,\omega)$:

$$\mathcal{E}_\theta(n,\omega) = -2\pi R Z(n,\omega) I(n,\omega) \ , \quad I(n,\omega) = \frac{iq\omega_0\lambda_n}{2\pi(\omega - n\omega_0)} \tag{16}$$

Wake voltage is given by inverse Laplace-Fourier transform,

$$V(\theta,t) = \sum_n e^{in\theta} \int_{\mathrm{Im}\ \omega = v} e^{-i\omega t} Z(n,\omega) I(n,\omega) \ , \quad v > 0 \ , \tag{17}$$

and the power is $\mathcal{P} = -dW/dt$, where W is the work done per unit time by the wake field,

$$\mathcal{P}(t) = q\omega_0 \sum_n e^{in\omega_0 t} \lambda_n^* \int_{\mathrm{Im}\ \omega = v} d\omega e^{-i\omega t} Z(n,\omega) I(n,\omega) \ . \tag{18}$$

Wake voltage and power spectrum - 1

To compute V and $\mathcal{P}$, move ω-contour to semicircle in lower half-plane. We encounter poles of Z at TE and TM resonant modes and also WG (wave guide) poles at the following frequencies and their negatives:

$$\begin{aligned}
\omega_{nps}^{TE} &= \frac{c}{b}\left[j_{ns}'^2 + (\alpha_p b)^2\right]^{1/2}, \quad s = 1, 2, \cdots \\
\omega_{nps}^{TM} &= \frac{c}{b}\left[j_{ns}^2 + (\alpha_p b)^2\right]^{1/2}, \quad s = 1, 2, \cdots \\
\omega_{p}^{WG} &= \alpha_p c
\end{aligned} \tag{19}$$

Wave guide poles from zeros of γ_p^2.

Label these frequencies by a multi-index j with values $(TE, n, p, s),\ (TM, n, p, s),\ (WG, p)$

We also encounter poles of $I(n, \omega)$ at frequencies $\omega = n\omega_0$.

Wake voltage: a new expression

Assuming that no ω_j coincides with one of the $n\omega_0$,

$$V(\theta,t) = \sum_n e^{in\omega_0}\int_{\mathrm{Im}\ \omega=v} d\omega e^{-i\omega t} Z(n,\omega) I(n,\omega)$$

$$= V_1(\theta-\omega_0 t) + V_2(\theta,t) = q\omega_0 \sum_n \lambda_n Z(n,n\omega_0) e^{in(\theta-\omega_0 t)}$$

$$+q\omega_0 \sum_n \lambda_n e^{in\theta} \sum_j \left[\frac{e^{-i\omega_j t}\mathrm{R}(n,\omega_j)}{\omega_j - n\omega_0} - \frac{e^{i\omega_j t}\mathrm{R}(n,-\omega_j)}{\omega_j + n\omega_0} \right].$$

The term V_1 from poles of $I(n,\omega)$ at $\omega = n\omega_0$ is the known expression, usually written with $Z(n,n\omega_0) = Z(n)$. It depends only on the distance from the reference particle and corresponds to waves with phase velocity equal to particle velocity.

If $n\omega_0$ should (accidentally) hit one of the ω_j, then V_1 and V_2 are separately infinite, but cancel to a finite result. The incorrect Fourier transform gives infinity!!

Discussion of new term in the wake voltage

The new term is a time-dependent wake, not depending only on the distance from the reference particle:

$$V_2(\theta, t) = q\omega_0 \sum_n e^{in\theta}\lambda_n \sum_j \left[\frac{e^{-i\omega_j t}\mathrm{R}(n, \omega_j)}{\omega_j - n\omega_0} - \frac{e^{i\omega_j t}\mathrm{R}(n, -\omega_j)}{\omega_j + n\omega_0} \right].$$

It represents various waves of incoherent frequencies moving in both directions. The corresponding term in the power oscillates in sign, so energy is leaving and entering the field.

But when wall resistance is included,

$$\lim_{t\to\infty} V_2(\theta, t) = 0 \tag{20}$$

In practice, ∞ is at most a few turns.

There is also a contribution from a branch point at $\omega = 0$ which vanishes as well in the limit. (Skin depth contains $\sqrt{\omega}$.)

Wake and power at large t with wall resistance

If Z is computed with wall resistance, as was done in W & M, then at large t,

$$V(\theta, t) = q\omega_0 \sum_n \lambda_n Z(n, n\omega_0) e^{in(\theta - \omega_0 t)}$$
$$P = q\omega_0 \sum_n |\lambda_n|^2 \mathrm{Re}\ Z(n, n\omega_0)\ . \qquad (21)$$

Power spectrum for SLAC damping ring parameters, resistive toroidal chamber: (each peak composed of many n with $n\omega_0 \approx \omega_r$; TE and TM alternate, $n = 23000 - 105000$)

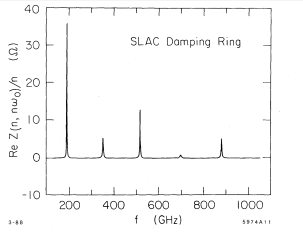

Forward from 1988 to 2007

e-mail from Jack Bergstrom, Canadian Light Source:

"Your ······ 1990 paper (with Morton) predicted that the radiation impedance of a closed "pillbox" dipole-magnet vacuum chamber should exhibit resonances, while the open parallel-plate model (used by most folks) of course does not. I think we are now seeing those resonances, both the TE and the TM modes, in our coherent-IR studies, just as your formalism predicts."

Who is Jack Bergstrom?

- Professor Emeritus, Nuclear Physics, University of Saskatchewan, 30 years of teaching
- Consultant for CLS, expert on instrumentation for storage rings, fast feedback, etc.
- Worked with Jeff Corbett on Australian Light Source, diagnostic beam line
- Acute eye for patterns in data, does extensive reading

CSR Spectra from Canadian Light Source (CLS) - 1

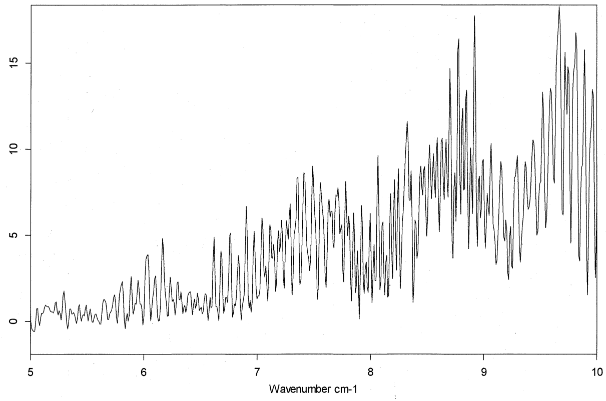

- Not noise! High resolution spectrum from Michelson interferometer, Bruker IFS 125 HR, resolution to $< 0.001 cm^{-1}$.

Bruker FTIR (Frustrated Total Internal Reflection) Spectrometer

Spectrometer

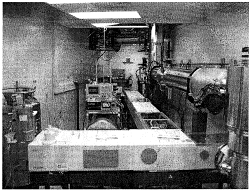

Bruker IFS 125 HR
Maximum Resolution: 0.00096 cm^{-1}

Beamsplitter	Spectral Range
Mylar 6 μm	30-630 cm^{-1}
Mylar 75 μm	12-35 cm^{-1}
Ge/KBr	400-4800 cm^{-1}
CaF_2	1850-20000 cm^{-1}
Detectors	
MCT N	600-10000 cm^{-1}
MCT B	450-10000 cm^{-1}
DTGS	100-3000 cm^{-1}
DTGS PE	15-700 cm^{-1}
Si Bolometer	10-370 cm^{-1}
Ge:Cu	300-1850 cm^{-1}
Internal	
Globar	10 – 13000 cm^{-1}
Hg – Lamp	10 – 1000 cm^{-1}
Tungsten Lamp	1000-25000 cm^{-1}

www.lightsource.

Beam is split, path length difference between two beams is scanned. Cosine Fourier transform of intensity vs. path difference gives power spectrum (real part of impedance times bunch spectrum).

CSR Spectra from Canadian Light Source (CLS) - 2

- Interferograms extremely invariant to changes in machine setup and optics: energy (1.5 - 2.9 GeV), fill pattern (single or multibunch), CSR in steady or bursting mode, bunch length (controlled by momentum compaction), IR optics, etc.
- Effect of optical instrumentation ruled out certainly. Big changes in the IR beam line optics, and replacement of the front end optics in the spectrometer, occurred over three years, but interferograms were unchanged!
- The number of peaks increases with increasing resolution.

  All this suggests that the peaks are resonances of the vacuum chamber, not affected by details of the beam.

Spectra at Brookhaven NSLS-VUV light source - 1

Bergstrom somehow associated the spiky graph in W & M with the CLS experimental spectrum. He made a quantitative fit of theoretical frequencies with CLS in a limited range, and later with NSLS-VUV data over a large range from

G. L. Carr, S. L. Kramer, N. Jisrawi, L. Mihaly, and D. Talbayev, Proc. 2001 Part. Accel. Conf., Chicago, p.377.

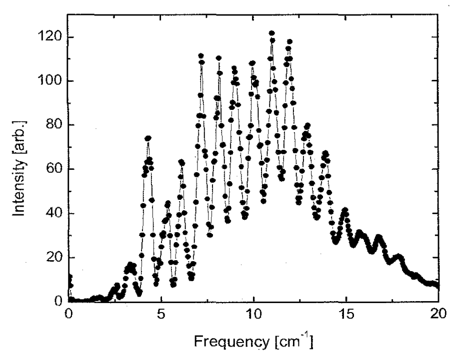

Spectra at Brookhaven NSLS-VUV light source - 2

High frequency data (CSR or ISR) from interferometer (Carr). Low frequency data (CSR) from microwave techniques - antenna, wave guides, frequency analyzer (Kramer).

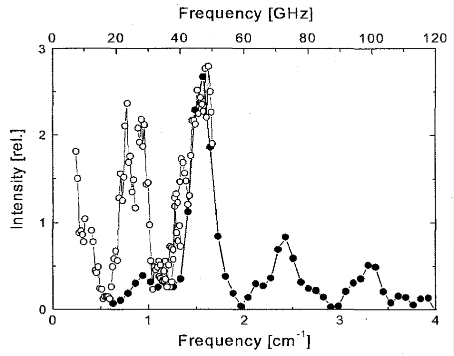

Figure: Black circles from interferometer, open circles from microwave techniques

Spectrum from toroidal (or pillbox) model of VUV chamber

Neglecting the straights, the VUV vacuum chamber is well modeled by a smooth torus with $w = 8$cm, $h = 4$cm. The bending radius $R = 1.91$m. I put the beam at $r = R$, and adjust the outer radius to $b = 1.948$m to fit the data; thus beam is 2mm off center.

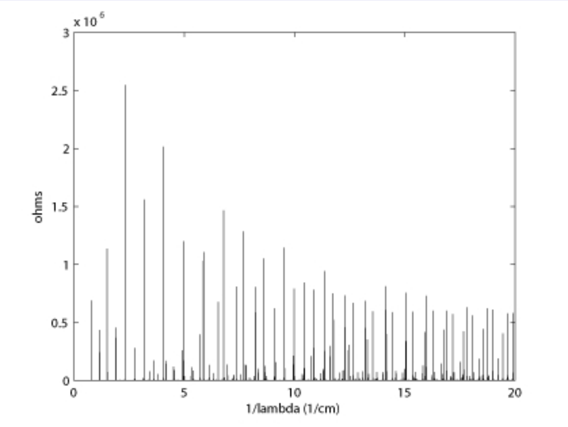

Comparison of VUV spectrum with experiment - 1

- Convolve theoretical spectrum with narrow Gaussian to average over small structures and perhaps imitate experimental resolution
- Compare frequencies of resulting smoothed spectrum to experiment, but do not worry about heights of peaks (influenced by optical beam line attenuation, bunch spectrum, resolution, etc.)

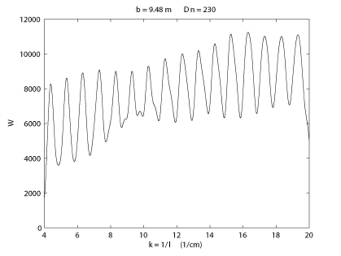

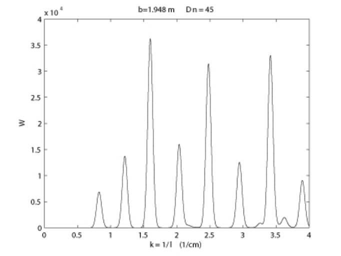

Figure: Theoretical spectrum convolved with narrow Gaussian

Comparison of VUV spectrum with experiment - 2

Table: Theoretical frequencies compared to data

Exp.	**Thy.**	**Exp.**	**Thy.**
0.80	0.827	6.10	6.31
0.93	—	7.25	7.32
1.32	1.21	9.00	8.32
1.57	1.60	10.0	9.29
2.10*	2.04	11.1	10.28
2.40	2.48	12.0	11.29
2.76*	2.94	12.8	12.33
3.10*	3.26	13.8	13.31
3.66*	3.62	15.0	14.3
3.88*	3.90	15.7-15.9	15.3
4.20	4.38	16.7	16.3
5.25	5.34	18.0	17.3
		18.8*	18.3

Comparison of VUV spectrum with experiment - 3

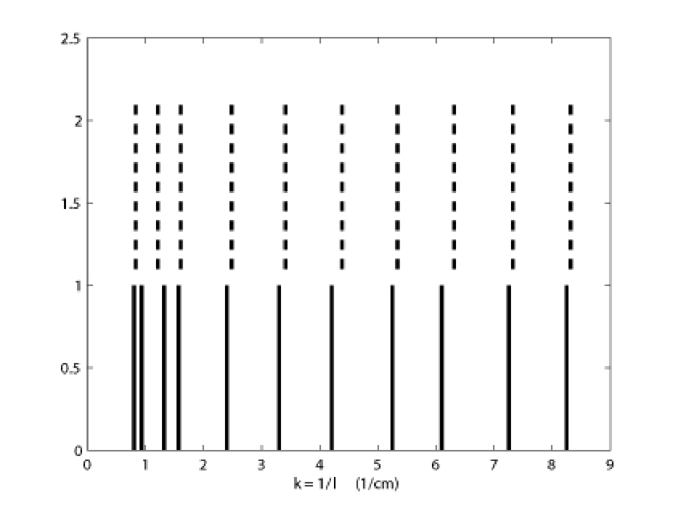

Figure: Comparison of experimental and theoretical spectra. Solid lines are from experiment, dashed lines from theory.

Comparison to experiment - discussion

- The experimental lines at $0.80\mathrm{cm}^{-1}$ and $0.93\mathrm{cm}^{-1}$ came from two different microwave bands (different wave guides, hence different normalization), and may not really correspond to two separate peaks (Kramer's comment). Anyway, they are close to the theoretical lowest mode, a TE, at $0.827\mathrm{cm}^{-1}$.
- The signal below the CSR threshold, $k < 0.5\mathrm{cm}^{-1}$, is associated with microwaves from a machine impedance due to bellows. This interpretation is consistent with a streak camera measurement.
- The experimental line at $1.32\mathrm{cm}^{-1}$ is precious to the comparison, since it corresponds to the only TM mode in the theory that really stands out after the smoothing by convolution. Kramer thinks this line is authentic, even though it was not seen by Carr's interferometer.

CLS dipole chamber - a challenge for theoretical modeling

The CLS has two special vacuum chamber structures at dipoles associated with IR beam lines, involving large excursions in the outer chamber wall.

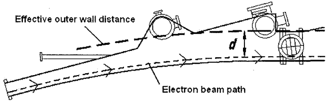

Figure 3: Top view of dipole chamber showing electron beam radius with arrows and distance d to the outer wall. M1 extraction mirror located in rectangular opening in chamber at right, outside of the magnet windings (not shown).

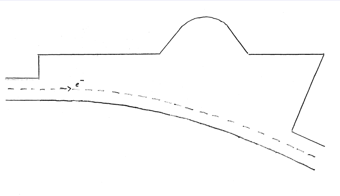

Figure: Flared vacuum chamber, "effective distance" from beam to wall $d = 21$cm, vs. 3.2cm in normal chamber of straights and other dipoles.

Fit to smooth chamber theory with effective chamber radius

Bergstrom could fit CLS spectrum over a limited frequency domain using the smooth chamber theory with $b = R + d, \; d = 21\text{cm}$.

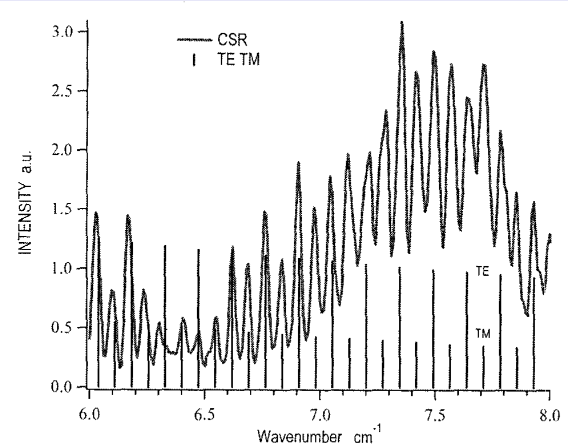

Experiment to modify vacuum chamber at CLS

CLS built an apparatus to modify the vacuum chamber by dropping a metallic tube, a “plunger” , through an existing vacuum port. Bergstrom made a heuristic calculation (lacking a satisfactory theory) predicting that a structure at 7cm path difference in the interferogram would change with the plunger in. An experiment gave a vague indication of the expected change, but needs to be repeated with a better signal-to-noise ratio.

The calculation: integrating the smooth chamber impedance with variable wall radius $b(\theta)$, over length of chamber.

Pillbox with a side box as a model of CLS dipole chambers

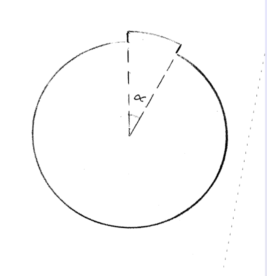

High frequency standing wave modes in the "cavity" expressed by Bessel functions of order $m\pi/\alpha$, large m. Through mode matching these can overlap with usual whispering gallery modes of the unperturbed pill box.

Expect some vestige of both pillbox and cavity modes in the solution, and excitation of resonances at any multiple of the revolution frequency, since all n-modes are coupled. Thus a much more complicated spectrum!

Equations for the side box model - 1

- Equations for E_z and H_z remain uncoupled.
- In the cavity region E_z, H_z expanded in $\sin(\hat{m}\theta)$, $\cos(\hat{m}\theta)$ with $\hat{m} = \pi m/\alpha$ to meet boundary conditions on end walls.
- To meet boundary conditions on outer wall at $r = b+ = b + d$, Laplace-Fourier coefficients have the form

$$\begin{aligned} E^c_{zmp}(r,\omega) &= a_{mp} p_{\hat{m}}(\gamma_p r, \gamma_p b+) \ , \\ H^c_{zmp}(r,\omega) &= c_{mp} q_{\hat{m}}(\gamma_p r, \gamma_p b+) \ . \end{aligned} \tag{22}$$

- Equations involve all the cross products, in general for non-integer order μ:

$$\begin{aligned} p_\mu(x,y) &= J_\mu(x)Y_\mu(y) - Y_\mu(x)J_\mu(y) \ , \\ q_\mu(x,y) &= J_\mu(x)Y'_\mu(y) - Y_\mu(x)J'_\mu(y) \ , \\ r_\mu(x,y) &= J'_\mu(x)Y_\mu(y) - Y'_\mu(x)J_\mu(y) \ , \\ s_\mu(x,y) &= J'_\mu(x)Y'_\mu(y) - Y'_\mu(x)J'_\mu(y) \ . \end{aligned} \tag{23}$$

Equations for the side box model - 2

The coefficients c_{mp} for H_z in the cavity satisfy the set of equations

$$q_{\hat{m}}(\gamma_p b, \gamma_p b+) c_{mp} = \sum_{m'} L(m, m') s_{\hat{m}'}(\gamma_p b, \gamma_p b+) c_{m'p} + \mathcal{S}_{mp} \ ,$$

$$L(m, m') = \frac{\alpha}{4\pi} \sum_n M_{mn} \frac{J_n(\gamma_p b)}{J_n'(\gamma_p b)} M^\dagger_{nm'} \ ,$$

$$M_{mn} = \frac{2}{\alpha} \int_0^\alpha e^{in\theta} \cos(\hat{m}\theta) d\theta \ , \tag{24}$$

with source term

$$\mathcal{S}_{mp} = \sum_n M_{mn} \left[h_{znp}(b) - \frac{J_n(\gamma_p b)}{\gamma_p J_n'(\gamma_p b)} h'_{znp}(b) \right] \ ,$$

$$h_{znp}(b) = \frac{\pi}{2} q H_p \lambda_n \gamma_p \beta c \ q_n(\gamma_p b, \gamma_p R) \frac{1}{2\pi i(\omega - n\omega_0)} \ . \tag{25}$$

Resonances given by zeros of the determinant. Field at the beam expressed in terms of c_{mp}, a_{mp}.

Structure of equations for the side box model - 1

- The source involves poles $1/(\omega - n\omega_0)$ for all n. Any harmonic of the revolution frequency can be excited, but the driving term is proportional to the overlap M_{mn} and is maximum for $\hat{m} = n$. This setup leads to a matrix impedance $Z(n, n', n'\omega_0)$ appearing in the wake voltage, with a sum on n' against $\lambda_{n'}$.
- Near a TE pillbox resonance, where $J_n'(\gamma_p b) = 0$, only one term in the kernel $L(m, m')$ is important. The system can then be solved analytically since its matrix is rank 1. Result: a resonance near the unperturbed pillbox resonance if the cavity is shallow.

Structure of equations for the side box model - 2

- The diagonal matrix elements of the system have zeros at frequencies almost equal to those of a sector chamber with radius $b+ = b + d$; that is where $J'_{\hat{m}}(\gamma_p b+) = 0$ for the TE case.
- If the perturbation from off-diagonal terms is not too large, we then have a vestige of sector chamber modes in the spectrum. This might explain Bergstrom's partial success in using a local average radius to fit the observed spectrum.

Summary

- Whispering gallery theory provides a plausible fit to VUV spectra. Further experiments at VUV would be welcome, since its vacuum chamber is nearly ideal.
- At CLS, the extreme stability of spectra to changes in the machine setup and IR optics suggests that spectra are determined by the vacuum chamber primarily.
- A theory in progress makes it unsurprising that the CLS spectra are more complicated that those of VUV, owing to large wall excursions in the IR vacuum chambers. The simple smooth gallery picture is strongly perturbed but not completely destroyed.

Outlook

Workshop at CLS on Nov. 1-2, 2010, to discuss possible EXPERIMENTS on CSR spectra.

Jack Bergstrom, Tim May, Brant Billinghurst *et al.*, CLS

Steve Kramer, NSLS

Peter Kuske and Martin Ries (for Gode Wüstefeld), BESSY, MLS

Anke-Suzanne Müller, ANKA

James Safranek, Bob Warnock, SLAC

Shane Koscielniak, TRIUMF

John Byrd (virtually?), ALS

Rui Li, JNAL

Jim Ellison (?), UNM

THEORY: Numerical solution of the side box model underway, and Vlasov solutions with Z of torus. Hope to get to real wall profile and inclusion of straights.